

1 Light rays

1.1 Light rays in human experience

The formation of an image is one of our most fascinating emotional experiences. Even in ancient times it was realized that our ‘vision’ is the result of rectilinearly propagating light rays, because everybody was aware of the sharp shadows of illuminated objects. Indeed, rectilinear propagation may be influenced by certain optical instruments, e.g. by mirrors or lenses. Following the successes of Tycho Brahe (1546–1601), knowledge about *geometrical optics* made for the consequential design and construction of magnifiers, microscopes and telescopes. All these instruments serve as aids to vision. Through their assistance, ‘insights’ have been gained that added to our world picture of natural science, because they enabled observations of the world of both micro- and macro-cosmos.

Thus it is not surprising that the terms and concepts of optics had tremendous impact on many areas of natural science. Even such a giant instrument as the new Large Hadron Collider (LHC) particle accelerator in Geneva is basically nothing other than an admittedly very elaborate microscope, with which we are able to observe the world of elementary particles on a subnuclear length scale. Perhaps as important for the humanities is the wave theoretical description of optics, which spun off from the development of quantum mechanics.

In our human experience, rectilinear propagation of light rays – in a homogeneous medium – stands in the foreground. But it is a rather newer understanding that our ability to see pictures is caused by an optical image in the eye.

Nevertheless, we can understand the formation of an image with the fundamentals of ray optics. That is why this textbook starts with a chapter on ray optics.



Fig. 1.1: *Light rays.*

1.2 Ray optics

When light rays spread spherically into all regions of a homogeneous medium, in general we think of an idealized, point-like and isotropic luminous source at their origin. Usually light sources do not fulfil any of these criteria. Not until we reach a large distance from the observer may we cut out a nearly parallel beam of rays with an aperture. Therefore, with an ordinary light source, we have to make a compromise between intensity and parallelism, to achieve a beam with small divergence. Nowadays optical demonstration experiments are nearly always performed with laser light sources, which offer a nearly perfectly parallel, intense optical beam to the experimenter.

When the rays of a beam are confined within only a small angle with a common optical axis, then the mathematical treatment of the propagation of the beam of rays may be greatly simplified by linearization within the so-called ‘paraxial approximation’. This situation is met so often in optics that properties such as those of a thin lens, which go beyond that situation, are called ‘aberrations’.

The direction of propagation of light rays is changed by refraction and reflection. These are caused by metallic and dielectric interfaces. Ray optics describes their effect through simple phenomenological rules.

1.3 Reflection

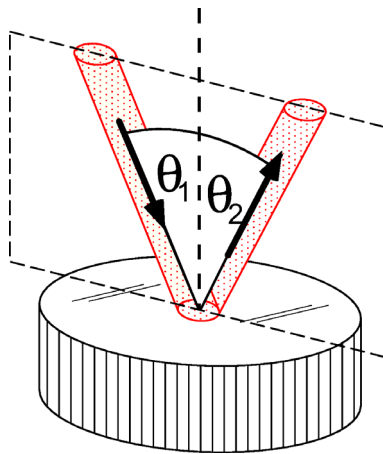


Fig. 1.2: Reflection at a planar mirror.

We observe reflection, or mirroring of light rays not only on smooth metallic surfaces, but also on glass plates and other dielectric interfaces. Modern mirrors may have many designs. In everyday life they mostly consist of a glass plate coated with a thin layer of evaporated aluminium. But if the application involves laser light, more often dielectric multilayer mirrors are used; we will discuss these in more detail in the chapter on interferometry (Chapter 5). For ray optics, the type of design does not play any role.

1.3.1 Planar mirrors

We know intuitively that at a planar mirror like in Fig. 1.2 the *angle of incidence* θ_1 is identical with the *angle of reflection* θ_2 of the reflected beam,

$$\theta_1 = \theta_2, \quad (1.1)$$

and that incident and reflected beams lie within a plane together with the surface normal. Wave optics finally gives us a more rigid reason for the laws of reflection. Thereby also details like, for example, the intensity ratios for dielectric reflection (Fig. 1.3) are explained, which cannot be derived by means of ray optics.

1.4 Refraction

At a planar dielectric surface, like e.g. a glass plate, reflection and transmission occur concurrently. Thereby the transmitted part of the incident beam is ‘refracted’. Its change of direction can be described by a single physical quantity, the ‘index of refraction’ (also: refractive index). It is higher in an optically ‘dense’ medium than in a ‘thinner’ one.

In ray optics a general description in terms of these quantities is sufficient to understand the action of important optical components. But the refractive index plays a key role in the context of the macroscopic physical properties of dielectric matter and their influence on the propagation of macroscopic optical waves as well. This interaction is discussed in more detail in the chapter on light and matter (Chapter 6).

1.4.1 Law of refraction

At the interface between an optical medium ‘1’ with refractive index n_1 and a medium ‘2’ with index n_2 (Fig. 1.3) Snell’s law of refraction (Willebrord Snell, 1580–1626) is valid,

$$n_1 \sin \theta_1 = n_2 \sin \theta_2, \quad (1.2)$$

where θ_1 and θ_2 are called the angle of incidence and angle of emergence at the interface. It is a bit artificial to define two absolute, material-specific refractive indices, because according to Eq. (1.2) only their ratio $n_{12} = n_1/n_2$ is determined at first. But considering the transition from medium ‘1’ into a third material ‘3’ with n_{13} , we realize that, since $n_{23} = n_{21}n_{13}$, we also know the properties of refraction at the transition from ‘2’ to ‘3’. We can prove this relation, for example by inserting a thin sheet of material ‘3’ between ‘1’ and ‘2’. Finally, fixing the refractive index of vacuum to $n_{\text{vac}} = 1$ – which is argued within the context of wave optics – the specific and absolute values for all dielectric media are determined.

In Tab. 1.1 on p. 9 we collect some physical properties of selected glasses. The refractive index of most glasses is close to $n_{\text{glass}} = 1.5$. Under usual atmospheric conditions the refractive index in air varies between 1.000 02 and 1.000 05. Therefore, using $n_{\text{air}} = 1$, the refraction

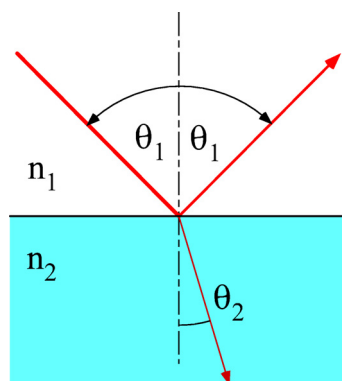


Fig. 1.3: Refraction and reflection at a dielectric surface.

properties of the most important optical interface, i.e. the glass–air interface, may be described adequately in terms of ray optics. Nevertheless, small deviations and variations of the refractive index may play an important role in everyday optical phenomena in the atmosphere (for example, fata morgana, p. 6).

1.4.2 Total internal reflection

According to Snell’s law, at the interface between a dense medium ‘1’ and a thinner medium ‘2’ ($n_1 > n_2$), the condition (1.2) can only be fulfilled for angles smaller than the critical angle θ_c ,

$$\theta < \theta_c = \sin^{-1}(n_2/n_1). \quad (1.3)$$

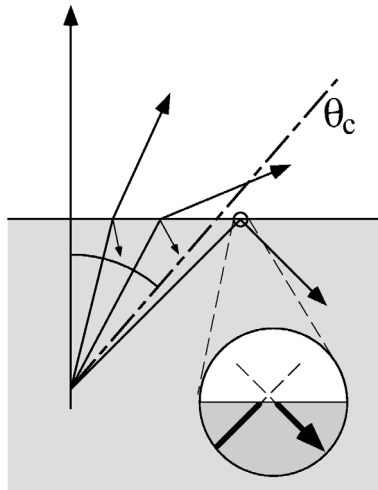


Fig. 1.4: Total internal reflection at a dielectric surface. The point of reflection of the rays does not lie exactly within the interface, but slightly beyond (the Goos–Haenchen effect [36, 88]).

For $\theta > \theta_c$ the incident intensity is totally reflected at the interface. We will see in the chapter on wave optics that light penetrates into the thinner medium for a distance of about one wavelength with the so-called ‘evanescent’ wave, and that the point of reflection does not lie exactly at the interface (Fig. 1.4). The existence of the evanescent wave enables the application of the so-called ‘frustrated’ total internal reflection, e.g. for the design of polarizers (Chapter 3.5.4).

1.5 Fermat’s principle: the optical pathlength

As long as light rays propagate in a homogeneous medium, they seem to follow the shortest geometric path from the source to a point, making their way in the shortest possible time. If refraction occurs along this route, then the light ray obviously no longer moves on the geometrically shortest path.

The French mathematician Pierre de Fermat (1601–1665) postulated in 1658 that in this case the light ray should obey a *minimum principle*, moving from the source to another point along the path that is *shortest in time*.

For an explanation of this principle, one cannot imagine a better one than that given by the American physicist Richard P. Feynman (1918–1988), who visualized

Fermat's principle with a human example: One may imagine Romeo discovering his great love Juliet at some distance from the shore of a shallow, leisurely flowing river, struggling for her life in the water. Without thinking, he runs straight towards his goal – although he might have saved valuable time if he had taken the longer route, running the greater part of the distance on dry land, where he would have achieved a much higher speed than in the water.

Considering this more formally, we determine the time required from the point of observation to the point of the drowning maiden as a function of the geometric pathlength. Thereby we find that the shortest time is achieved exactly when a path is chosen that is refracted at the water–land boundary. It fulfils the refraction law (1.2) exactly, if we substitute the indices of refraction n_1 and n_2 by the inverse velocities in water and on land, i.e.

$$\frac{n_1}{n_2} = \frac{v_2}{v_1}.$$

According to Fermat's minimum principle, we have to demand the following. The propagation velocity of light in a dielectric c_n is reduced in comparison with the velocity in vacuum c by the refractive index n :

$$c_n = c/n.$$

Now the *optical pathlength* along a trajectory \mathcal{C} , where the refractive index n depends on the position \mathbf{r} , can be defined in general as

$$\mathcal{L}_{\text{opt}} = c \int_{\mathcal{C}} \frac{ds}{c/n(\mathbf{r})} = \int_{\mathcal{C}} n(\mathbf{r}) ds. \quad (1.4)$$

With the tangential unit vector \mathbf{e}_t , the path element $ds = \mathbf{e}_t \cdot d\mathbf{r}$ along the path can be calculated.

Example: Fermat's principle and refraction

As an example of the use of the integral principle, we will again consider refraction at a dielectric surface and therefore vary the length of the optical path between the points A and B in Fig. 1.5 (\mathbf{r}_{AO} = vector from A to O etc., $\mathbf{e}_{1,2}$ = unit vectors),

$$\begin{aligned} \mathcal{L}_{\text{opt}} &= n_1 \mathbf{e}_1 \cdot \mathbf{r}_{AO} + n_2 \mathbf{e}_2 \cdot \mathbf{r}_{OB}, \\ d\mathcal{L}_{\text{opt}} &= (n_1 \mathbf{e}_1 - n_2 \mathbf{e}_2) \cdot d\mathbf{r}. \end{aligned}$$

Now varying only the distance along the surface (\mathbf{N} = surface normal) and taking into account $d\mathbf{r} \perp \mathbf{N}$, we can specify the condition

$$(n_1 \mathbf{e}_1 - n_2 \mathbf{e}_2) \times \mathbf{N} = 0,$$

which is a vectorial formulation of Snell's law (1.2) reproducing it at once.

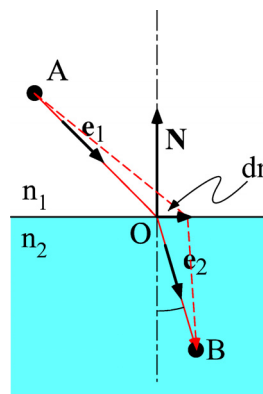


Fig. 1.5: Fermat's principle and refraction at a dielectric surface.

1.5.1 Inhomogeneous refractive index

In general, the index of refraction of a body is not spatially homogeneous, but has underlying, continuous, even though small, fluctuations like the material itself, which affect the propagation of light rays: $n = n(\mathbf{r})$. We observe such fluctuations in, for example, the flickering of hot air above a flame. From the phenomenon of mirages, we know that efficient reflection may arise like in the case of grazing incidence at a glass plate, even though the refractive index decreases only a little bit towards the hot bottom.

Again using the idea of the integral principle, this case of propagation of a light ray may also be treated by applying Fermat's principle. The contribution of a path element ds to the optical pathlength is $d\mathcal{L}_{\text{opt}} = n ds = n \mathbf{e}_t \cdot d\mathbf{r}$, where $\mathbf{e}_t = d\mathbf{r}/ds$ is the tangential unit vector of the trajectory. On the other hand $d\mathcal{L}_{\text{opt}} = \nabla \mathcal{L}_{\text{opt}} \cdot d\mathbf{r}$ is valid in accordance with Eq. (1.4), which yields the relation

$$n \mathbf{e}_t = n \frac{d\mathbf{r}}{ds} = \nabla \mathcal{L}_{\text{opt}} \quad \text{and} \quad n^2 = (\nabla \mathcal{L}_{\text{opt}})^2,$$

which is known as the *eikonal equation* in optics. We get the important *ray equation* of optics, by differentiating the eikonal equation after the path¹,

$$\frac{d}{ds} \left(n \frac{d\mathbf{r}}{ds} \right) = \nabla n. \quad (1.5)$$

A linear equation may be reproduced for homogeneous materials ($\nabla n = 0$) from (1.5) without difficulty.

Example: Fata morgana

As a short example we will treat reflection at a hot film of air near the ground, which induces a decrease in air density and thereby a reduction of the refractive index. (Another example is the propagation of light rays in a gradient waveguide – section 1.7.3.) We may assume in good approximation that for calm air the index of refraction increases with distance y from the bottom, e.g. $n(y) = n_0(1 - \varepsilon e^{-\alpha y})$. Since the effect is small, $\varepsilon \ll 1$ is valid in general, while the scale length α is of the order $\alpha = 1 \text{ m}^{-1}$. We look at Eq. (1.5) for $\mathbf{r} = (y(x), x)$ for all individual components and find for the x coordinate with constant C

$$n \frac{dx}{ds} = C.$$

We may use this result as a partial parametric solution for the y coordinate,

$$\frac{d}{ds} \left(n \frac{dy}{ds} \right) = \frac{d}{dx} \left(n \frac{dy}{dx} \frac{dx}{ds} \right) \frac{dx}{ds} = \frac{d}{dx} \left(C \frac{dy}{dx} \right) \frac{C}{n} = \frac{\partial n(y)}{\partial y}.$$

¹Thereby we apply $d/ds = \mathbf{e}_t \cdot \nabla$ and

$$\frac{d}{ds} \nabla \mathcal{L} = (\mathbf{e}_t \cdot \nabla) \nabla \mathcal{L} = \frac{1}{n} (\nabla \mathcal{L} \cdot \nabla) \nabla \mathcal{L} = \frac{1}{2n} \nabla (\nabla \mathcal{L})^2 = \frac{1}{2n} \nabla n^2.$$

The constant may be chosen to be $C = 1$, because it is only scaling the x coordinate. Since $2n \partial n / \partial y = \partial n^2 / \partial y$ and $n^2 \simeq n_0^2(1 - 2\varepsilon e^{-\alpha y})$, we get for $\varepsilon \ll 1$

$$\frac{d^2 y(x)}{dx^2} = \frac{1}{2} \frac{\partial}{\partial y} n^2(y) = n_0^2 \varepsilon \alpha e^{-\alpha y}.$$

This equation can be solved by fundamental methods and it is convenient to write the solution in the form

$$y = y_0 + \frac{1}{\alpha} \ln [\cosh^2(\kappa(x - x_0))] \xrightarrow{\kappa(x-x_0) \gg 1} y_0 + \frac{2\kappa}{\alpha}(x - x_0).$$

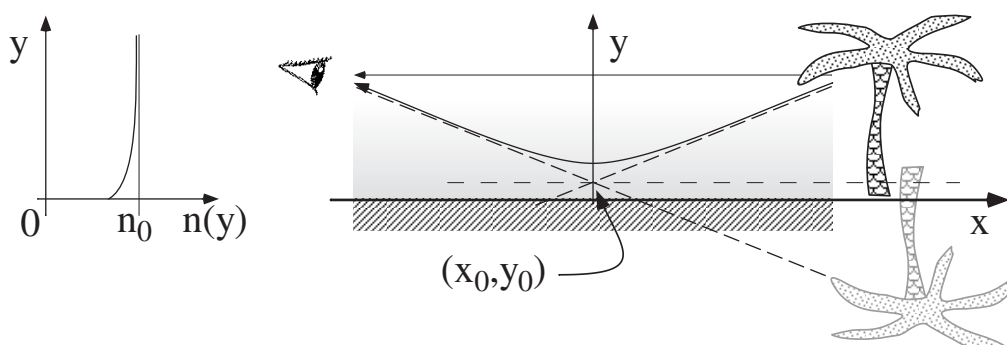


Fig. 1.6: Profile of the refractive index and optical path for a fata morgana.

For large distances from the point of reflection at $x = x_0$ we find straight propagation as expected. The maximum angle $\phi = \arctan(2\kappa/\alpha)$, where reflection is still possible, is defined by $\kappa \leq n_0 \alpha (\varepsilon/2)^{1/2}$. As in Fig. 1.6 the observer registers two images – one of them is upside down and corresponds to a mirror image. The curvature of the light rays declines quickly with increasing distance from the bottom and therefore may be neglected for the ‘upper’ line of sight. At (x_0, y_0) a ‘virtual’ point of reflection may be defined.

1.6 Prisms

The technically important rectangular reflection is achieved with an angle of incidence of $\theta_i = 45^\circ$. For ordinary glasses ($n \simeq 1.5$), this is above the angle of total internal reflection $\theta_c = \sin^{-1} 1.5 = 42^\circ$. Glass prisms are therefore often used as simple optical elements, which are applied for beam deflection. More complicated prisms are realized in many designs for multiple reflections, where they have advantages over the corresponding mirror combinations due to their minor losses and more compact and robust designs.

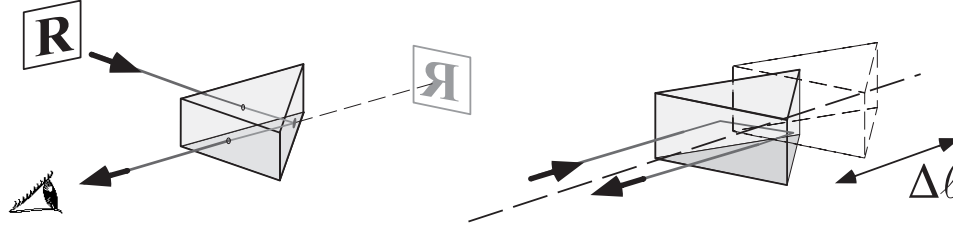


Fig. 1.7: Reflection or 90° prism. This prism is used for rectangular beam deflection. It may also be used for the design of a retroreflector, whereby an optical delay $\Delta t = \Delta \ell / c$ is realized by simple adjustment.

Often used designs are the Porro prism and the retroreflector (Fig. 1.8) – other names for the latter are ‘corner cube reflector’, ‘cat’s eye’ or ‘triple mirror’. The Porro prism and its variants are applied for example in telescopes to create upright images. The retroreflector not only plays an important role in optical distance measurement techniques and interferometry, but also enables functioning of security reflectors - cast in plastics - in vehicles.

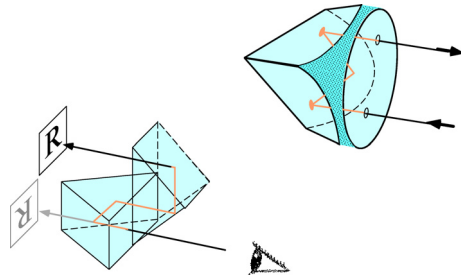


Fig. 1.8: The Porro prism (left) is combined out of two rectangular prisms, which rotate the image plane of an object such that in combination with lenses one gets an upright image. The retroreflector (right) throws back every light ray independently of its angle of incidence, but causing a parallel shift.

We may also regard cylindrical glass rods as a variant of prisms where total internal reflection plays an important role. In such a rod (see Fig. 1.11) a light ray is reflected back from the surface to the interior again and again, without changing its path angle relative to the rod axis. Such fibre rods are used, for example, to guide light from a source towards a photodetector. In miniaturized form they are applied as *waveguides* in optical telecommunications. Their properties will be discussed in the section on beam propagation in waveguides (Section 1.7) and later on in the chapter on wave optics (Chapter 3.3)

in more detail.

1.6.1 Dispersion

Prisms played a historical role in the spectral decomposition of white light into its constituents. The refractive index and thus also the angle of deflection δ in Fig. 1.9 actually depend on the wavelength, $n = n(\lambda)$, and therefore light rays of different colours are deflected with different angles. Under *normal dispersion* blue wavelengths are refracted more strongly than red, $n(\lambda_{\text{blue}}) > n(\lambda_{\text{red}})$.

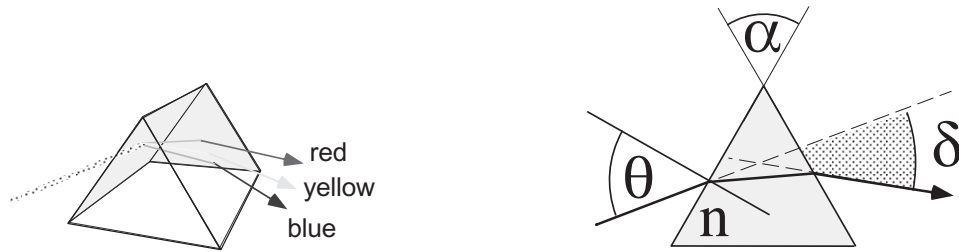


Fig. 1.9: Refraction and dispersion at a symmetrical prism. The index of refraction n can be calculated from the minimum angle of deflection $\delta = \delta_{\min}$ in a simple manner.

Refractive index and dispersion are very important technical quantities for the application of optical materials. The refractive index is tabulated in manufacturers' data sheets for various wavelengths, and (numerous different) empirical formulae are used for the wavelength dependence. The constants from Tab. 1.1 are valid for the formula which is also called *Sellmeier equation*:

$$n^2 = 1 + \frac{B_1\lambda^2}{\lambda^2 - C_1} + \frac{B_2\lambda^2}{\lambda^2 - C_2} + \frac{B_3\lambda^2}{\lambda^2 - C_3} \quad (\lambda \text{ in } \mu\text{m}). \quad (1.6)$$

Tab. 1.1: Optical properties of selected glasses.

Name	Boron crown	Heavy flint glass		Barium crown	Flint glass
Abbreviation	BK7	SF11	LaSF N9	BaK 1	F 2
Abbé number A	64.17	25.76	32.17	57.55	36.37
Refractive index n for selected wavelengths					
$\lambda = 486.1 \text{ nm}$	1.5224	1.8065	1.8690	1.5794	1.6321
$\lambda = 587.6 \text{ nm}$	1.5168	1.7847	1.8503	1.5725	1.6200
$\lambda = 656.3 \text{ nm}$	1.5143	1.7760	1.8426	1.5695	1.6150
Dispersion constants of refractive index (see Eq. 1.6)					
B_1	1.0396	1.7385	1.9789	1.1237	1.3453
B_2	0.2379	0.3112	0.3204	0.3093	0.2091
B_3	1.0105	1.1749	1.9290	0.8815	0.9374
C_1	0.0060	0.0136	0.0119	0.0064	0.0100
C_2	0.0200	0.0616	0.0528	0.0222	0.0470
C_3	103.56	121.92	166.26	107.30	111.89
Density ρ (g cm^{-3})					
	2.51	4.74	4.44	3.19	3.61
Expansion coefficient $\Delta\ell/\ell$ (-30 to $+70^\circ\text{C}$) $\times 10^6$					
	7.1	6.1	7.4	7.6	8.2

Strain birefringence: typically 10 nm cm^{-1} .

Homogeneity of the refractive index from melt to melt: $\delta n/n = \pm 1 \times 10^{-4}$.

By geometrical considerations we find that the angle of deflection δ in Fig. 1.9 depends not only on the angle of incidence θ but also on the aperture angle α of the symmetrical prism and of course on the index of refraction, n ,

$$\begin{aligned}\delta &= \alpha - \theta + \arcsin \left[\cos \alpha \sin \theta - \sin(\alpha \sqrt{n^2 - \sin^2 \theta}) \right], \\ \delta_{\min} &= \alpha - 2\theta_{\text{symm}}.\end{aligned}$$

The minimum deflection angle δ_{\min} is achieved for symmetrical transit through the prism and enables a precise determination of the refractive index. The final result is expressed straightforwardly by the quantities α and δ_{\min} ,

$$n = \frac{\sin [(\alpha + \delta_{\min})/2]}{\sin (\alpha/2)}.$$

For quantitative estimation of the dispersive power K of glasses, the Abbe number A may be used. This relates the refractive index at a yellow wavelength (at $\lambda = 587.6$ nm, the D line of helium) to the change of the refractive index, estimated from the difference of the refractive indices at a blue ($\lambda = 486.1$ nm, Fraunhofer line F of hydrogen) and a red wavelength ($\lambda = 656.3$ nm, Fraunhofer line C of hydrogen),

$$A = K^{-1} = \frac{n_{\text{D}} - 1}{n_{\text{F}} - n_{\text{C}}}.$$

According to the above, a large Abbe number means weak dispersion, and a small Abbe number means strong dispersion. The Abbe number is also important when correcting chromatic aberrations (see Chapter 4.5.3).

The index of refraction describes the interaction of light with matter, and we will come to realize that it is a complex quantity, which describes not only the properties of dispersion but also those of absorption as well. Furthermore, it is the task of a microscopic description of matter to determine the dynamic polarizability and thus to establish the connection to a macroscopic description.

1.7 Light rays in waveguides

The transmission of messages via light signals is a very convenient method that has a very long history of application. For example, in the 19th century, mechanical pointers were mounted onto high towers and were observed with telescopes to realize transmission lines of many hundreds of miles. An example of a historic relay station from the 400 mile Berlin-Cologne-Coblenz transmission line is shown in Fig.1.10. Basically, in-air transmission is also performed nowadays, but with laser light. But it is always affected by its scattering properties even at small distances, because turbulence, dust and rain can easily inhibit the propagation of a free laser beam.

Ideas for guiding optical waves have been in existence for a very long time. In analogy to microwave techniques, for example, at first hollow tubes made of copper were applied, but their attenuation is too large for transmission over long distances. Later on periodical lens systems have been used for the same purpose, but due to high losses and small mechanical flexibility they also failed.

The striking breakthrough happened to ‘optical telecommunication’ through the development of low-loss *waveguides*, which are nothing other than elements for guiding light rays. They can be distributed like electrical cables, provided that adequate transmitters and receivers are available. With overseas cables, significantly shorter signal transit times and thus higher comfort for phone calls can be achieved than via geostationary satellites, where there is always a short but unpleasant and unnatural break between question and answer.

Therefore, propagation of light rays in dielectric waveguides is an important chapter in modern optics. Some basics may yet be understood by the methods of ray optics.



Fig. 1.10: *Historic station No. 51 of the Berlin–Cologne–Coblenz optic-mechanical ‘sight’ transmission line on the tower of the St. Pantaleon church, Cologne. Picture from Weiger (1840).*

1.7.1 Ray optics in waveguides

Total internal reflection in an optically thick medium provides the fundamental physical phenomenon for guiding light rays within a dielectric medium. Owing to this effect, for example, in cylindrical homogeneous glass fibres, rays whose angle with the cylinder axis stays smaller than the angle of total internal reflection θ_c are guided from one end to the other. Guiding of light rays in a homogeneous glass cylinder is affected by any distortion of the surface, and a protective cladding could even suppress total internal reflection.

Therefore, various concepts have been developed, where the optical waves are guided in the centre of a waveguide through variation of the index of refraction. These waveguides may be surrounded by cladding and entrenched like electrical cables.

We will present the two most important types. Step-index fibres consist of two homogeneous cylinders with different refractive indices (Fig. 1.11). To achieve beam guiding, the higher index of refraction must be in the cladding. Gradient-index fibres with continuously changing (in good approximation, parabolic) refractive index are more sophisticated to manufacture, but they have technical advantages like, for example, a smaller group velocity dispersion.

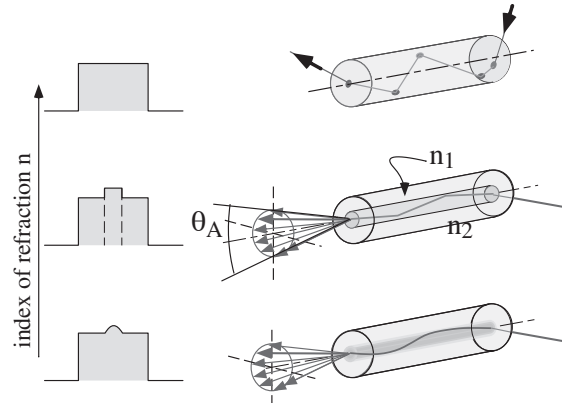


Fig. 1.11: Profiles of the refractive index and ray path in optical waveguides. Upper: waveguide with homogeneous refractive index. Centre: waveguide with stepped profile of refractive index (step-index fibre). Lower: waveguide with continuous profile of refractive index (gradient-index fibre).

Excursion: Manufacturing waveguides

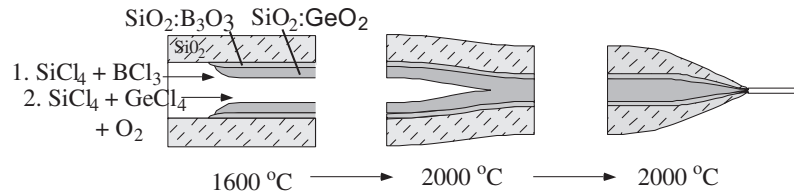


Fig. 1.12: Manufacturing of waveguides. The preform is manufactured with appropriate materials with distinct indices of refraction, which are deposited on the inner walls of a quartz tube by a chemical reaction.

The starting material is an ordinary tube made of quartz glass. It rotates on a lathe and is blown through on the inside by a gas mixture (chlorides like highly purified SiCl_4 , GeCl_4 , etc.). A oxyhydrogen burner heats a small zone of only a few inches up to about 1600°C , in which the desired materials are deposited as oxides on the inner walls (*chemical vapour deposition, CVD*). Thus by multiple repetition a refractive index profile is established, before the tube is melted at about 2000°C to a massive glass rod of about 10 mm diameter, a so-called preform. In the last step a fibre pulling machine extracts the glass fibre out of a crucible with viscous material. Typical cross-sections are 50 and $125\ \mu\text{m}$, which are coated with a cladding for protection.

1.7.2 Step-index fibres

The principle of total internal reflection is applied in *step-index fibres* (Fig. 1.13), which consist of a *core* with refractive index n_1 and a *cladding* with $n_2 < n_1$. The

relative difference in the index of refraction

$$\Delta = \frac{n_1 - n_2}{n_1} \quad (1.7)$$

is not more than 1–2%, and the light rays are only guided if the angle α towards the fibre axis is shallow enough to fulfil the condition for total internal reflection.

For example, for quartz glass ($n_2 = 1.45$ at $\lambda = 1.55 \mu\text{m}$), whose core index of refraction has been enhanced by GeO_2 doping up to $n_1 = n_2 + 0.015$, according to $\theta_c = \sin^{-1}(n_2/n_1)$ one finds the critical angle $\theta_c = 81.8^\circ$. The complementary beam angle relative to the fibre axis, $\alpha_G = 90^\circ - \theta_c$, can be approximated by

$$\alpha_G \simeq \sin \alpha_G \simeq \sqrt{2\Delta},$$

since $n_2/n_1 = 1 - \Delta$, and thus is set in relation to Δ , which yields $\alpha \leq 8.2^\circ$ for this case.

When light rays cross the axis of a fibre, propagation takes place in a cut plane, which is called the *meridional plane*. *Skewed rays* pass through the axis and are guided on a polygon around the circle. It can be shown that the rays must confine an angle $\alpha < \alpha_G$ with the z axis to be guided by total internal reflection.

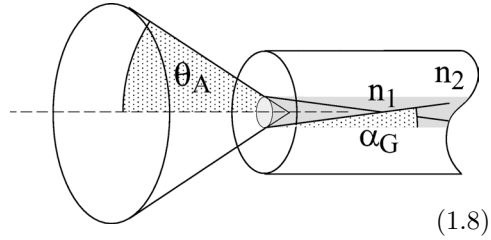


Fig. 1.13: Critical angle in a step-index fibre.

Numerical aperture of an optical fibre

To guide a light ray in an optical fibre, the angle of incidence at the incoupler must be chosen small enough. The maximum aperture angle θ_a of the acceptance cone can be calculated according to the refraction law, $\sin \theta_a = n_1 \sin \alpha_G = n_1 \cos \theta_c$. The sine of the aperture angle is called the numerical aperture (NA). According to Eq. (1.8) and $\cos \theta_c \simeq \sqrt{2\Delta}$ it can be related with the physical parameters of the optical fibre,

$$\text{NA} = n_1 \sqrt{2\Delta}. \quad (1.9)$$

This yields, for example, $\text{NA} = 0.21$ for the quartz glass fibre mentioned above, which is a useful and typical value for standard waveguides.

Propagation velocity

Light within the core of the waveguide propagates along the trajectory with a velocity $v(r(z)) = c/n(r(z))$. Along the z axis the beam propagates with a reduced velocity, $\langle v_z \rangle = v \cos \alpha$, which can be calculated for small angles $\alpha(z)$ to the z axis according to

$$\langle v_z \rangle \simeq \frac{c}{n_1} \left(1 - \frac{1}{2} \alpha^2 \right). \quad (1.10)$$

In Chapter 3.3 on the wave theory of light, we will see that the propagation velocity is identical with the group velocity.

1.7.3 Gradient-index fibres

Beam guiding can also be performed by means of a *gradient-index fibre* (GRIN), where the quadratic variation of the index of refraction is important. To determine the curvature of a light ray induced by the refractive index, we apply the ray equation (1.5). This is greatly simplified in the paraxial approximation ($ds \simeq dz$) and for a cylindrically symmetric fibre,

$$\frac{d^2 r}{dz^2} = \frac{1}{n} \frac{dn}{dr}.$$

A parabolic profile of the refractive index with a difference of the refractive index of $\Delta = (n_1 - n_2)/n_1$,

$$n(r \leq a) = n_1 \left[1 - \Delta \left(\frac{r}{a} \right)^2 \right] \quad \text{and} \quad n(r > a) = n_2, \quad (1.11)$$

decreases from the maximum value n_1 at $r = 0$ to n_2 at $r = a$. One ends up with the equation of motion of a harmonic oscillator,

$$\frac{d^2 r}{dz^2} + \frac{2\Delta}{a^2} r = 0,$$

and realizes immediately that the light ray performs oscillatory motion about the z axis. The period is

$$\Lambda = \frac{2\pi a}{\sqrt{2\Delta}}, \quad (1.12)$$

and a light ray is described with a wavenumber $K = 2\pi/\Lambda$ according to

$$r(z) = r_0 \sin(2\pi z/\Lambda).$$

The maximum elongation allowed is $r_0 = a$, because otherwise the beam loses its guiding. Thereby also the maximum angle $\alpha_G = \sqrt{2\Delta}$ for crossing the axis occurs. It is identical with the critical angle for total internal reflection in a step-index fibre and yields also the same relation to the numerical aperture (Eq. (1.9)). As in the case of a step-index fibre, the propagation velocity of the light ray is of interest. Using the approximation eq. (1.10) we calculate the average velocity during an oscillation period with $\tan \alpha \simeq \alpha = dr(z)/dz$,

$$\langle v_z \rangle = \left\langle \frac{c \cos \alpha(r(z))}{n(r(z))} \right\rangle = \frac{c}{n_1} \left\langle \frac{1 - \Delta(r_0/a)^2 \cos^2(Kz)}{1 - \Delta(r_0/a)^2 \sin^2(Kz)} \right\rangle,$$

and find after a short conversion the remarkable result

$$\langle v_z \rangle = \frac{c}{n_1} \left[1 - \left(\frac{\Delta}{2} \right)^2 \left(\frac{\alpha}{\alpha_G} \right)^2 \right],$$

which actually means that, because $\Delta \ll 1$, the propagation velocity within a gradient-index fibre depends much less on the angle α than that within a step-index fibre. As we will see, this circumstance plays an important role for signal propagation in waveguides (see Chapter 3.3).

1.8 Lenses and curved mirrors

The formation of an image plays a major role in optics, and *lenses* and *curved mirrors* are essential parts in optical devices. First we will discuss the effect of these components on the propagation of rays; owing to its great importance we have dedicated an extra chapter (Chapter 4) to the formation of images.

1.8.1 Lenses

We define an *ideal* lens as an optical element that merges all rays of a point-like source into one point again. An image where all possible object points are transferred into image points is called a *stigmatic* image (from the Greek: *stigma*, point). The source may even be far away and illuminate the lens with a parallel bundle of rays. In this case the point of merger is called the *focal point* or *focus*. In Fig. 1.14, we consider a beam of parallel rays that passes through the lens and is merged in the focal point. According to Fermat's principle, the optical pathlength must be equal for all possible paths, which means that they are independent from the distance of a partial beam from the axis. Then the propagation of light must be delayed most on the symmetry axis and less and less at the outer areas!

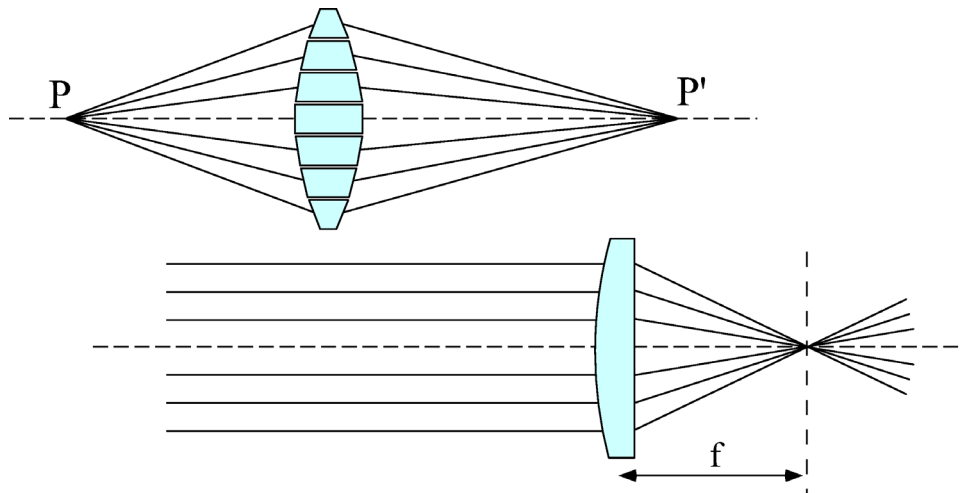


Fig. 1.14: Upper: Stigmatic lens imaging. All rays starting at object point P are merged again at image point P' . The light rays are delayed more near the axis of the lens body than in the outermost areas, so that all rays make the same optical pathlength to the image point. A lens may be figured as a combination of several prisms. Lower: A parallel beam of rays originating from a source at infinite distance is focused at the focal point at focal distance f .

For a simplified analysis, we neglect the thickness of the lens body, consider the geometrical increase of the pathlength from the lens to the focal point at a distance f

and expand the term as a function of distance r from the axis,

$$\ell(r) = \sqrt{f^2 + r^2} \simeq f \left(1 + \frac{r^2}{2f^2} \right). \quad (1.13)$$

To compensate for the quadratic increase of the optical pathlength $\ell(r)$, the delay by the path within the lens glass – i.e. the thickness – must also vary quadratically. This is actually the condition for spherical surfaces, which have been shown to be extremely successful for convergent lenses! The result is the same with much more mathematical effort, if one explores the properties of refraction at a lens surface assuming that a lens is constructed of many thin prisms (Fig. 1.14). In the chapter on lens aberrations, we will deal with the question of which criteria should be important for the choice of a planar convex or biconvex lens.

1.8.2 Concave mirrors

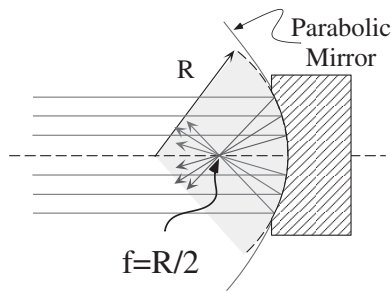


Fig. 1.15: Path of rays for a concave mirror. For near-axis incident light, spherical mirrors are used.

Among curved mirrors, concave or parabolic mirrors play the most important role. They are very well known from huge astronomical telescopes (see Chapter 4), because we entered the fascinating world of the cosmos with their aid. But they are used much more often in laser resonators (Chapter 5.6).

Taking into account the tangential plane at the intercept of the surface normal at the lens surface, we can transfer the conditions of planar reflection to curved mirror surfaces. Concave mirrors mostly have axial symmetry, and the effect on a parallel beam of rays within one cut plane is visualized in Fig. 1.15.

The reflected partial rays meet at the focal point or focus on the mirror axis, as they do in the case of a lens. It is known from geometry that the reflection points must then lie on a parabola. Near the axis, parabolic mirrors may in good approximation be substituted by spherical mirrors, which are much easier to manufacture. On the left-hand side of Fig. 1.16 the geometrical elements are shown, out of which the dependence of the focal length (defined here by the intersection point with the optical axis) on the axis distance y_0 of a parallel incident beam may be calculated,

$$f = R - \frac{R}{2 \cos \alpha} \simeq \frac{R}{2} \left[1 - \frac{1}{2} \left(\frac{y_0}{R} \right)^2 + \dots \right].$$

In general we neglect the quadratic correction, which causes an aperture error and is investigated in more detail in Chapter 4.5.2.

In laser resonators a situation often occurs in which spherical mirrors are simultaneously used as deflection mirrors, e.g. in the ‘bowtie resonator’ in Fig. 7.35. Then the

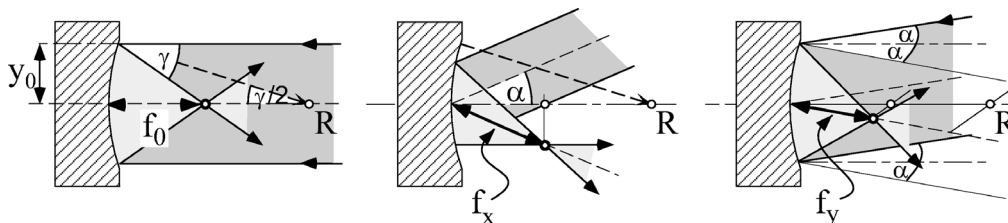


Fig. 1.16: Focusing an incident beam that is parallel to (left) and oblique to (centre: top view; right: side view) the optical axis.

focal width of the rays within the ray plane (f_x) and within the plane perpendicular to that one (f_y) will differ from $f_0 = R/2$,

$$f_x = \frac{R}{2 \cos \alpha} = \frac{f_0}{\cos \alpha} \quad \text{and} \quad f_y = \frac{R \cos \alpha}{2} = f_0 \cos \alpha.$$

The geometrical situations in the top view (Fig. 1.16, centre) are easy to see. In the side view one looks at the projection onto a plane perpendicular to the direction of emergence. The projections of the radius and focal length are reduced to $R \cos \alpha$ and $f \cos \alpha$, respectively. The difference between the two planes occurring here is called astigmatic aberration and sometimes can be compensated by simple means (see for example p. 126).

1.9 Matrix optics

As a result of its rectilinear propagation, a free light ray may be treated like a straight line. In optics, systems with axial symmetry are especially important, and an individual light ray may be described sufficiently well by the distance from and angle to the axis (Fig. 1.17). If the system is not rotationally symmetric, for example after passing through a cylindrical lens, then we can deal with two independent contributions in the x and y directions with the same method.

The modification of the beam direction by optical components – mirrors, lenses, dielectric surfaces – is described by a trigonometric and therefore not always simple relation. For near-axis rays, these functions can often be linearized, and thus the mathematical treatment is simplified enormously. This becomes obvious, for example, for a linearized form of the law of refraction (1.2):

$$n_1 \theta_1 = n_2 \theta_2. \quad (1.14)$$

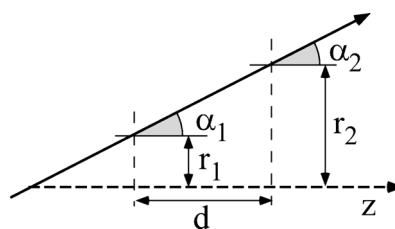


Fig. 1.17: Key variables of an optical ray for simple translation.

Here we have made use of this approximation already with the application of Fermat's principle for ideal lenses. Near-axis rays allow the application of spherical surfaces for lenses, which are much easier to manufacture than mathematical ideal surfaces. Furthermore, ideal systems are only 'ideal' for selected ray systems, otherwise they suffer from image aberrations like other systems.

When treating the modification of a light ray by optical elements in this approximation by linear transformation, matrices are a convenient mathematical tool for calculating the fundamental properties of optical systems. The development of this method made for the denomination *matrix optics*. The introduction of transformation matrices for ray optics may be visualized very easily, but they achieved striking importance, because they do not change their form when treating near-axis rays according to wave optics (see section 2.3.2). Furthermore this formalism is also applicable for other types of optics like 'electron optics', or the even more general 'particle optics'.

1.9.1 Paraxial approximation

Let us consider the propagation of a light ray at a small angle α to the z axis. The beam is fully determined by the distance r from the z axis and the slope $r' = \tan \alpha$. Within the so-called *paraxial approximation*, we now linearize the tangent of the angle and substitute it by its argument, $r' \simeq \alpha$, and then merge r with r' to end up with a vector $\mathbf{r} = (r, \alpha)$. At the start a light ray may have a distance to the axis and a slope of $\mathbf{r}_1 = (r_1, \alpha_1)$. Having passed a distance d along the z axis, then

$$\begin{aligned} r_2 &= r_1 + \alpha_1 d, \\ \alpha_2 &= \alpha_1, \end{aligned}$$

holds. One may use 2×2 matrices to write the translation clearly,

$$\mathbf{r}_2 = \mathbf{T} \mathbf{r}_1 = \begin{pmatrix} 1 & d \\ 0 & 1 \end{pmatrix} \mathbf{r}_1. \quad (1.15)$$

A bit more complicated is the modification by a refracting optical surface. For that purpose we look at the situation of Fig. 1.18, where two optical media with refractive indices n_1 and n_2 are separated by a spherical interface with radius R . If the radius vector subtends an angle ϕ with the z axis, then the light ray is obviously incident on the surface at an angle $\theta_1 = \alpha_1 + \phi$ and is related to the angle of emergence by the law of refraction.

In paraxial approximation according to Eq. (1.2), $n_1 \theta_1 \simeq n_2 \theta_2$ and $\phi \simeq r_1/R$ is valid, and one finds

$$n_1 \left(\alpha_1 + \frac{r_1}{R} \right) = n_2 \left(\alpha_2 + \frac{r_2}{R} \right).$$

The linearized relations may be described easily by the refraction matrix \mathbf{B} ,

$$\begin{pmatrix} r_2 \\ \alpha_2 \end{pmatrix} = \mathbf{B} \begin{pmatrix} r_1 \\ \alpha_1 \end{pmatrix} = \begin{pmatrix} 1 & 0 \\ (n_1 - n_2)/n_2 R & n_1/n_2 \end{pmatrix} \begin{pmatrix} r_1 \\ \alpha_1 \end{pmatrix}. \quad (1.16)$$

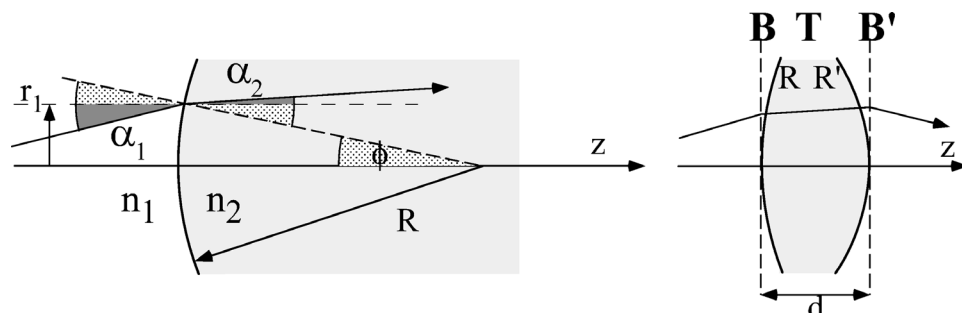


Fig. 1.18: Modification of a light ray at curved refracting surfaces.

1.9.2 ABCD matrices

The most important optical elements may be specified by their transformations, also called *ABCD matrices*,

$$\begin{pmatrix} r_2 \\ \alpha_2 \end{pmatrix} = \begin{pmatrix} A & B \\ C & D \end{pmatrix} \begin{pmatrix} r_1 \\ \alpha_1 \end{pmatrix}, \quad (1.17)$$

which we collect in Tab. 1.2 for look-up purposes and will be presented in the following in more detail.

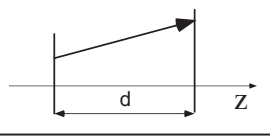
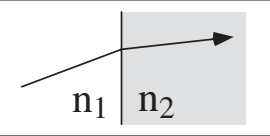
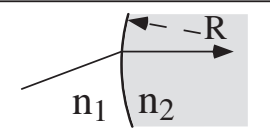
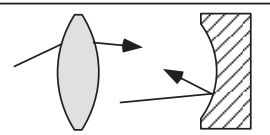
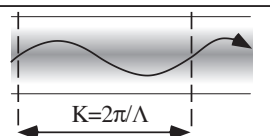
According to Fig. 1.18 the effect of a lens on a light ray is characterized by a refraction \mathbf{B} at the entrance, a translation \mathbf{T} in the glass and one further refraction \mathbf{B}' at the exit. Now the matrix method shows its strength, because the effect of a lens can easily be expressed as a product $\mathbf{L} = \mathbf{B}'\mathbf{T}\mathbf{B}$ of three operations,

$$\begin{pmatrix} r_2 \\ \alpha_2 \end{pmatrix} = \mathbf{L} \begin{pmatrix} r_1 \\ \alpha_1 \end{pmatrix} = \mathbf{B}'\mathbf{T}\mathbf{B} \begin{pmatrix} r_1 \\ \alpha_1 \end{pmatrix}. \quad (1.18)$$

Before we discuss the lens and some more examples in detail, we have to fix some conventions, which in general are used in matrix optics:

1. The ray direction goes from left to right in the positive direction of the z axis.
2. The radius of a convex surface is positive, $R > 0$, and that of a concave surface is negative, $R < 0$.
3. The slope is positive when the beam moves away from the axis, and negative when it moves towards the axis.
4. An object distance or image distance is positive (negative) when lying in front of (behind) the optical element.
5. Object distances are defined to be positive (negative) above (below) the z axis.
6. Reflective optics is treated by flipping the ray path after every element.

Tab. 1.2: Important ABCD matrices.

Operation		ABCD-Matrix
Translation		$\begin{pmatrix} 1 & d \\ 0 & 1 \end{pmatrix}$
Refraction (planar surface)		$\begin{pmatrix} 1 & 0 \\ 0 & n_1/n_2 \end{pmatrix}$
Refraction (curved surface)		$\begin{pmatrix} 1 & 0 \\ \frac{n_1-n_2}{n_2 R} & \frac{n_1}{n_2} \end{pmatrix}$
Lenses Curved Mirrors (focal length f)		$\begin{pmatrix} 1 & 0 \\ -1/f & 1 \end{pmatrix}$
Optical Fiber GRIN (length ℓ)		$\begin{pmatrix} \cos K\ell & K^{-1}\sin K\ell \\ -K\sin K\ell & \cos K\ell \end{pmatrix}$

1.9.3 Lenses in air

Now we will explicitly calculate the lens matrix \mathbf{L} according to eq. (1.18) and we take into account the index of refraction $n_{\text{air}} = 1$ in Eqs. (1.15) and (1.16). The expression

$$\mathbf{L} = \begin{pmatrix} 1 - \frac{n-1}{n} \frac{d}{R} & \frac{d}{n} \\ (n-1) \left[\frac{1}{R'} - \frac{1}{R} - \frac{d(n-1)^2}{RR'n} \right] & 1 + \frac{n-1}{n} \frac{d}{R'} \end{pmatrix}$$

makes a complicated and not very convenient expression at first sight. Though it may allow the treatment of very thick lenses, by far the most important are the predominantly used ‘thin’ lenses, whose thickness d is small compared to the radii of curvature R , R' of the surfaces. With d/R , $d/R' \ll 1$ or by direct multiplication $\mathbf{B}'\mathbf{B}$, we find the much simpler form

$$\mathbf{L} \simeq \begin{pmatrix} 1 & 0 \\ (n-1) \left(\frac{1}{R'} - \frac{1}{R} \right) & 1 \end{pmatrix}$$

and introduce the symbol \mathcal{D} for the *refractive power* in the lensmaker’s equation ,

$$\mathcal{D} = -(n-1) \left(\frac{1}{R'} - \frac{1}{R} \right) = \frac{1}{f}. \quad (1.19)$$

Thus the ABCD matrix for thin lenses becomes very simple

$$\mathbf{L} = \begin{pmatrix} 1 & 0 \\ -\mathcal{D} & 1 \end{pmatrix} = \begin{pmatrix} 1 & 0 \\ -\frac{1}{f} & 1 \end{pmatrix}, \quad (1.20)$$

where the sign is chosen such that convergent lenses have a positive refractive power. The refractive power is identical with the inverse focal length, $\mathcal{D} = 1/f$. The refractive power \mathcal{D} is measured in units of dioptres ($1 \text{ dpt} = 1 \text{ m}^{-1}$).

To support the interpretation of Eq. (1.20), we consider a bundle of rays that originates from a point source G on the z axis (Fig. 1.19). Such a bundle of rays can be described at a distance g from the source according to

$$\begin{pmatrix} r \\ \alpha \end{pmatrix} = \alpha \begin{pmatrix} g \\ 1 \end{pmatrix}. \quad (1.21)$$

We calculate the effect of the lens in the form

$$\mathbf{L} \begin{pmatrix} r \\ \alpha \end{pmatrix} = \alpha \begin{pmatrix} g \\ 1 - g/f \end{pmatrix} = \alpha' \begin{pmatrix} -b \\ 1 \end{pmatrix}. \quad (1.22)$$

The lens transforms the incident bundle of rays into a new bundle, which again has the form (1.21). It converges for $\alpha' < 0$ to the axis, crosses it at a distance $b > 0$ (convention 4) behind the lens, and creates there an image of the point source. If $b < 0$, then the virtual image of the point source lies in front of the lens and the lens has the properties of a dispersive lens.

By comparison of coefficients, we obtain the relation between object distance g and image distance b from Eq. (1.22) for lens imaging:

$$\frac{1}{f} = \frac{1}{g} + \frac{1}{b}. \quad (1.23)$$

This equation is the known basis for optical imaging. We refer to this topic again in Chapter 4 in more detail.

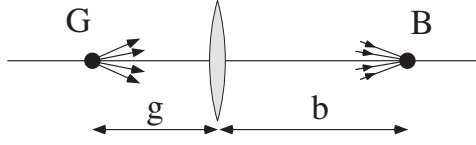


Fig. 1.19: Point image formation with a lens.

Example: ABCD matrix of an imaging system

For imaging by an arbitrary ABCD system, we must claim that a bundle of rays (r_1, α_1) is again merged at a point at a certain distance $d = d_1 + d_2$:

$$\begin{pmatrix} r_2 \\ \alpha_2 \end{pmatrix} = \begin{pmatrix} 1 & d_1 \\ 0 & 1 \end{pmatrix} \begin{pmatrix} A & B \\ C & D \end{pmatrix} \begin{pmatrix} 1 & d_2 \\ 0 & 1 \end{pmatrix} \begin{pmatrix} r_1 \\ \alpha_1 \end{pmatrix}.$$

For stigmatic imaging r_2 must be independent of α_1 and by calculation one finds the condition $d_1 D + d_2 A + d_1 d_2 C + B = 0$, which for $B = 0$ can be fulfilled by suitable choice of d_1 and d_2 , even if $C < 0$. Thus the ABCD matrix takes exactly the form that we know already from lenses and lens systems.

1.9.4 Lens systems

The matrix method enables us to explore the effect of a system consisting of two lenses with focal lengths f_1 and f_2 at a distance d . We multiply the ABCD matrices according to Eqs. (1.20) and (1.15) and get the matrix \mathbf{M} of the system

$$\begin{aligned} \mathbf{M} = \mathbf{L}_2 \mathbf{T} \mathbf{L}_1 &= \begin{pmatrix} 1 & 0 \\ -1/f_2 & 1 \end{pmatrix} \begin{pmatrix} 1 & d \\ 0 & 1 \end{pmatrix} \begin{pmatrix} 1 & 0 \\ -1/f_1 & 1 \end{pmatrix} \\ &= \begin{pmatrix} 1 - \frac{d}{f_1} & d \\ -\left(\frac{1}{f_2} + \frac{1}{f_1} - \frac{d}{f_1 f_2}\right) & 1 - \frac{d}{f_2} \end{pmatrix}. \end{aligned} \quad (1.24)$$

The system of two lenses substitutes a single lens with focal length given by

$$\frac{1}{f} = \frac{1}{f_2} + \frac{1}{f_1} - \frac{d}{f_1 f_2}. \quad (1.25)$$

We consider the following two interesting extreme cases.

- (i) $d \ll f_{1,2}$: Two lenses that are mounted directly next to each other, with no space between them, add their refractive powers, $\mathbf{M} \simeq \mathbf{L}_2 \mathbf{L}_1$ with $\mathcal{D} = \mathcal{D}_1 + \mathcal{D}_2$. This circumstance is used for example when adjusting eyeglasses, when refractive powers are combined until the required correction is found. Obviously a biconvex lens can be constructed out of two planar convex lenses, expecting that the focal length of the system is divided by two.
- (ii) $d = f_1 + f_2$: If the focal points coincide, a telescope is realized. A parallel bundle of rays with radius r_1 is widened or collimated into a new bundle of parallel rays with a new diameter $(f_2/f_1)r_1$. The refractive power of the system vanishes according to eq. (1.25), $\mathcal{D} = 0$. Such systems are called *afocal*.

A thin lens is one of the oldest optical instruments, and thin lenses may have many different designs due to their various applications. But since lens aberrations are of major interest, we will dedicate a specific chapter to the various designs (Chapter 4.5.1).

1.9.5 Periodic lens systems

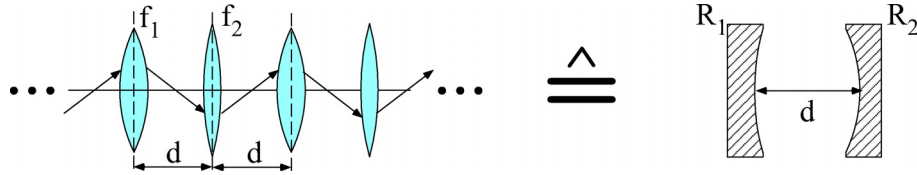


Fig. 1.20: Periodic lens system and equivalence to a two-mirror resonator.

Periodic lens systems had already been analysed in early times to realize optical light transmission lines. For such an application it is important that a light ray does not

leave the system even after long distances. We consider a periodic variant of the lens system with focal lengths f_1 and f_2 at a distance d . For that purpose we add one more identical translation to the transformation matrix from Eq. (1.24), which yields a system equivalent to a system of two concave mirrors (Fig. 1.20):

$$\begin{aligned} \begin{pmatrix} A & B \\ C & D \end{pmatrix} &= \begin{pmatrix} 1 & 0 \\ -1/f_2 & 1 \end{pmatrix} \begin{pmatrix} 1 & d \\ 0 & 1 \end{pmatrix} \begin{pmatrix} 1 & 0 \\ -1/f_1 & 1 \end{pmatrix} \begin{pmatrix} 1 & d \\ 0 & 1 \end{pmatrix} \\ &= \begin{pmatrix} 1 & d \\ -1/f_2 & 1-d/f_2 \end{pmatrix} \begin{pmatrix} 1 & d \\ -1/f_1 & 1-d/f_1 \end{pmatrix}. \end{aligned}$$

Now for n -fold application the individual element will cause total transformation

$$\begin{pmatrix} A_n & B_n \\ C_n & D_n \end{pmatrix} = \begin{pmatrix} A & B \\ C & D \end{pmatrix}^n.$$

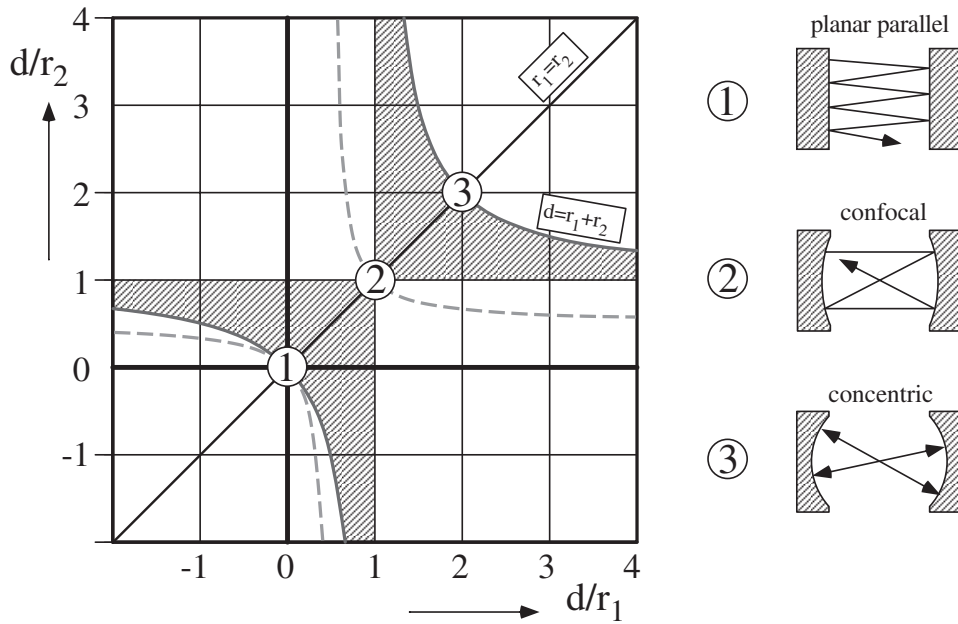


Fig. 1.21: Stability diagram for lenses and optical resonators according to the condition (1.27). Stable resonator configurations are within the hatched area. The dashed lines indicate the positions of confocal resonators, $d = (r_1 + r_2)/2$. Symmetric planar parallel, confocal and concentric resonators are at the positions circled 1, 2 and 3.

Introducing

$$\cos \Theta = \frac{1}{2}(A + D) = 2 \left(1 - \frac{d}{2f_1}\right) \left(1 - \frac{d}{2f_2}\right) - 1, \quad (1.26)$$

this matrix can be evaluated algebraically. Thus one calculates

$$\begin{pmatrix} A & B \\ C & D \end{pmatrix}^n = \frac{1}{\sin \Theta} \begin{pmatrix} A \sin n\Theta - \sin(n-1)\Theta & B \sin n\Theta \\ C \sin n\Theta & D \sin n\Theta - \sin(n-1)\Theta \end{pmatrix}.$$

The angle Θ must remain real, to avoid the matrix coefficients increasing to infinity. Otherwise the light ray would actually leave the lens system. Thus from the properties of the cosine function,

$$-1 \leq \cos \Theta \leq 1,$$

and in combination with Eq. (1.26) we get

$$0 \leq \left(1 - \frac{d}{2f_1}\right) \left(1 - \frac{d}{2f_2}\right) \leq 1. \quad (1.27)$$

This result defines a stability criterion for the application of a waveguide consisting of lens systems, and the corresponding important stability diagram is shown in Fig. 1.21. We will deal with this in more detail later on, because multiple reflection between concave mirrors of an optical resonator can be described in this way as well (Chapter 5.6).

1.9.6 ABCD matrices for waveguides

According to Section 1.7 and with the aid of the wavenumber constant $K = 2\pi/\Lambda$ (Eq. (1.12)) a simple ABCD matrix for the transformation of a ray by a graded-index fibre of length ℓ can be specified:

$$\mathbf{G} = \begin{pmatrix} \cos K\ell & K^{-1} \sin K\ell \\ -K \sin K\ell & \cos K\ell \end{pmatrix}. \quad (1.28)$$

With short pieces of fibre ($K\ell < \pi/4$) also thin lenses can be realized, and it can be shown that the focal point lies at $f = K^{-1} \cot K\ell$. These components are called *GRIN lenses*.

1.10 Ray optics and particle optics

Traditional optics, which deals with light rays and is the topic of this textbook, was conceptually in every respect a role model for ‘particle optics’, which started around the year 1900 with the exploration of electron beams and radioactive rays. Since ray optics describes the propagation of light rays, it is convenient to look for analogies in the trajectories of particles. We will see in the chapter on coherence and interferometry (Chapter 5) that the wave aspects of particle beams are widely coined in terms of the ideas of optics as well.

To re-establish the analogy explicitly, we refer to considerations about Fermat’s principle (p. 4), because there a relation between the velocity of light and the index of refraction is described. This relation is particularly simple if a particle moves in a conservative potential (potential energy $E_{\text{pot}}(\mathbf{r})$), like for example an electron in an electric field. As a result of energy conservation,

$$E_{\text{kin}}(\mathbf{r}) + E_{\text{pot}}(\mathbf{r}) = E_{\text{tot}},$$

we can immediately infer from $E_{\text{kin}} = mv^2/2$ that

$$v(\mathbf{r}) = \sqrt{\frac{2}{m}[E_{\text{tot}} - E_{\text{pot}}(\mathbf{r})]},$$

if the particles do not move too fast and we can adopt classical Newtonian mechanics (in a particle accelerator, the special theory of relativity has to be applied.).

We can define an effective relative index of refraction by

$$\frac{v(\mathbf{r}_1)}{v(\mathbf{r}_2)} = \frac{n_{\text{eff}}(\mathbf{r}_2)}{n_{\text{eff}}(\mathbf{r}_1)} = \frac{\sqrt{[E_{\text{tot}} - E_{\text{pot}}(\mathbf{r}_2)]}}{\sqrt{[E_{\text{tot}} - E_{\text{pot}}(\mathbf{r}_1)]}}.$$

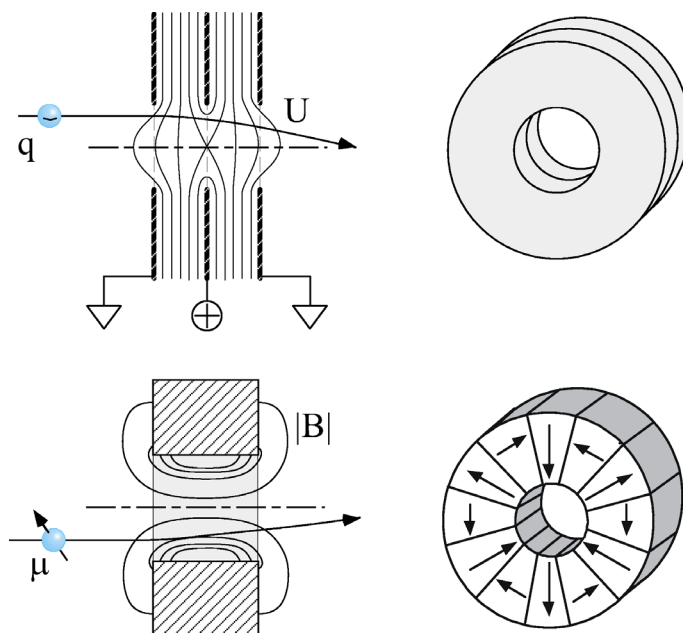


Fig. 1.22: Lenses for particle optics. Upper: So-called ‘single lens’ for electron optics with equipotential surfaces qU [81]. The potential is created by symmetric positioning of three conducting electrodes, the two outer ones lying on the same potential. Lower: Magnetic lens for atom optics with equipotential surfaces $|\mu \cdot B|$ [53]. An axial magnetic hexapole is formed out of circle segments, which are manufactured from a homogeneously magnetized permanent magnet (e.g. NdFeB or SmCo). The strength of the magnetic field rises as a square function of the radial distance.

As in the case of light, it must satisfy an additional condition, to be defined absolutely. For example, we may claim that $n_{\text{eff}} = 1$ for $E_{\text{pot}} = 0$. But then it is obvious that n_{eff} depends extremely on the velocity outside of the potential – particle optics has properties that are very much chromatic! The fundamental reason for this difference is the different relation between kinetic energy E and momentum p for light and for

particles having mass, which is also called the *dispersion relation*:

$$\begin{array}{ll} \text{Light} & E = pc, \\ \text{Particles} & E = p^2/2m. \end{array}$$

In charged particle beams a narrow velocity distribution can be created by acceleration, which makes the difference not very pronounced. But the broadness of the velocity distribution in thermal beams of neutral atoms induces significant problems. Indeed, this velocity distribution can be manipulated by so-called supersonic jets or by laser cooling (see Chapter 11.6) in such a way that even ‘atom optics’ can be established [53]. We present some important devices of electron and atom optics in Fig. 1.22.